Advanced Powder Technology xxx (2016) xxx–xxx

Contents lists available at ScienceDirect

Advanced Powder Technology

journal homepage: www.elsevier.com/locate/apt

Original Research Paper

Preparation, characterization and potential use of flower shaped Zinc oxide nanoparticles (ZON) for the adsorption of Victoria Blue B dye from aqueous solution

Navish Kataria [a], V.K. Garg [a,b,*], Monika Jain [a], K. Kadirvelu [c]

[a] Department of Environmental Science and Engineering, Guru Jambheshwar University of Science and Technology, Hisar 125001, India
[b] Centre for Environmental Sciences and Technology, Central University of Punjab, Bathinda 151001, Punjab, India
[c] DRDO BU Centre for Life Sciences, Bharathiar University Campus, Coimbatore 641046, Tamil Nadu, India

ARTICLE INFO

Article history:
Received 5 January 2016
Received in revised form 28 March 2016
Accepted 4 April 2016
Available online xxxx

Keywords:
Flower-shaped ZON
Victoria Blue B dye
Adsorption
Kinetics
Thermodynamics

ABSTRACT

In present work, the performance and effectiveness of flower-shaped Zinc oxide nanoparticles (ZON) synthesised by hydrothermal method was evaluated for the adsorption of Victoria Blue B (VB B) dye from aqueous solution. ZON were characterised by using XRD, FTIR, SEM, EDX and DLS. Batch mode adsorption experiments were carried out to optimise the process conditions viz., pH, adsorbent dose, dye concentration, temperature, etc. The adsorption of cationic dye onto ZON surface was illustrated by Langmuir and Temkin isotherm models. The mechanism of dye adsorption onto the nanoparticles was explained by pseudo-second order kinetic model ($R^2 \geqslant 0.997$). The thermodynamic parameters including Gibb's free energy (ΔG^0), enthalpy (ΔH^0), and entropy (ΔS^0) were studied at different temperatures (10–70 °C). The maximum adsorption capacity of VB B dye onto ZON was achieved up to 163 mg/g at pH 6.0 and temperature 27 ± 1 °C.

1. Introduction

The water pollution caused by organic (dyes) and inorganic (heavy metals) pollutants is of utmost importance because of their toxic and carcinogenic effects on living system including human beings. Therefore there is an urgent need to remove these contaminants from water and wastewaters keeping in view the stringent rules and regulation laid down by national and international agencies. The dye containing wastewaters are produced from various industries such as textile, pulp & paper, plastic and leather which pose significant environmental issues and problems [1,2]. The industrial wastewater containing synthetic organic dyes may be toxic, carcinogenic, teratogenic and mutagenic in nature for human as well as aquatic ecosystem [3].

VB B dye is a basic dye and belongs to class of triarylmethane dyes, it is widely used for anionic fabrics such as, cotton, silk and nylon. VB B dye is also used in quantitative estimation of phospholipids in thin layer chromatography [4]. VB B dye showed photocytotoxic effect and antitumour activity in some mammalian cell lines system [5]. Textile, pharmaceutical industry and municipal wastewaters are major source to expose the aquatic and human life to VB B dye. VB B dye causes toxicity in wastewater which has chronic effect on eye and respiratory system. [6].

Several approaches including adsorption [7], coagulation [8], membrane-filtration [9], photo-catalysis [10], ozonation, and oxidation [11] have been reported for the removal of dyes from wastewater. Each method has its own advantages and disadvantages like higher cost, sludge production and low regeneration capacity but adsorption being a conventional method is used broadly as it is cost effective, eco-friendly and easy to use. In past, various adsorbents like activated carbon [12], chitosan [13], agro-industrial wastes [14] and naturally occurring materials [15] have been used for adsorption of dyes. Nowadays, rapid advancement in nanotechnology has encouraged the scientific community to use various kinds of nanomaterials for the adsorption of pollutants from wastewater due to their smaller size, larger surface area, higher regeneration capacity, reusability, thermal stability and magnetic properties. Use of metal based oxide nanomaterials, viz., Fe_3O_4, TiO_2, Al_2O_3, MgO, SnO_2 has been reported for the removal of synthetic dyes and other environmental pollutants from aqueous medium [16,17]. Some other Zn containing

* Corresponding author at: Department of Environmental Science and Engineering, Guru Jambheshwar University of Science and Technology, Hisar 125001, India. Tel.: +91 9812058109.
E-mail address: vinodkgarg@yahoo.com (V.K. Garg).

http://dx.doi.org/10.1016/j.apt.2016.04.001
0921-8831/

nanoadsorbents for the adsorption of dyes from aqueous solution have been reported in literature. In this study, removal of VB B dye by ZON under varying process parameters (pH, initial dye concentration, adsorbent dose, temperature, agitation speed) in batch mode have been explored.

2. Experiments

2.1. Materials & reagents

Zinc nitrate hexahydrate [$Zn(NO_3)_3{\cdot}6H_2O$] and hexamethylenetetramine (HMTA) [$(CH_2)_6N_4$] was procured from Himedia laboratory Pvt. Ltd., India. Sodium hydroxide (NaOH) pellets (AR grade) and Victoria Blue B dye were procured from SD fine-chem Ltd, Mumbai. All chemicals used in the study were of AR grade. The physico-chemical characteristics of VB B dye are given in Table 1.

2.2. Synthesis of flower shaped Zinc oxide nanoparticles

ZON was synthesized by hydrothermal method. Zinc nitrate (0.1 M) solution and hexamethylenetetramine (0.1 M) solution were prepared in 100 mL double distilled water separately. Both solutions were mixed together at room temperature under vigorous stirring for 30 min and then 1 M NaOH solution was added drop wise in the above solution to raise the pH up to 10. The obtained milky slurry was refluxed at 80 °C for 7 h, after which white precipitates were formed. The laboratory synthesized precipitates were washed several times with double distilled water or ethanol and finally dried in a hot air oven at 60 °C for 3 h. The ZON were stored for further use in air tight plastic container.

2.3. Characterisation and apparatus

The structure of ZON was recorded by XRD (PANalytical X'Pert Pro Multipurpose Diffractometer powered by a Philips PW3040/60 X-ray generator, Netherlands), fitted with X'Celerator detector, using Cu K_α X-ray radiation (λ = 1.5418 Å) at 40 kV and a current of 40 mA. The average diameter of obtained particles suspension was analysed using dynamic light scattering (DLS) technique to record the size distribution by intensity spectra in a Zetasizer (Malvern, UK). The FTIR spectrum of the sample was recorded using FTIR (Thermo Scientific Nicolet 6700 FT-IR spectrometer, USA). The sample was mixed with spectral grade KBr for pelleting and was used for the FTIR analysis. The surface morphology and elemental characteristics of sample determined by Scanning electron microscope (SEM) and Energy-dispersive X-ray spectroscopy (EDX) techniques respectively, using ICON-Quanta 200 Mark II Environmental Scanning Electron Microscope.

2.4. Adsorption experiments

All the batch mode adsorption experiments for the removal of VB B dye by ZON were carried out in laboratory. The pH of dye solution was determined by cyber scan pH tutor (Eutech Instruments, Singapore). Dye concentration was analysed by UV–VIS spectrophotometer (UV–VIS 3000$^+$ LABINDIA, India). The experiments were conducted in 250 mL Erlenmeyer flasks with 100 mL of dye solution of desired concentration, at required contact time and adsorbent dose at a temperature of 27 ± 1 °C and stirring speed of 180 rpm (under dark condition). The adsorption experiments were done to optimise various process parameters i.e. pH, dye concentration, adsorbent dose, time, temperature, etc. The concentration or absorbance of dye solution before and after the experiments was detected by UV–VIS spectrophotometer at 599 nm. The wavelength of maximum absorption (λ_{max}) was determined by UV–VIS spectrophotometer. Dye removal (%) was calculated by the following expression:

$$\text{Dye removal } (\%) = \frac{(C_o - C_e)}{C_o} \times 100 \quad (1)$$

where C_o is the initial concentration and C_e is the equilibrium dye concentration in mg/L. The amount of dye adsorbed per unit of the adsorbent at equilibrium was calculated in terms of q_e (mg/g) using equation given below

$$\text{Adsorption capacity } (q_e) = \frac{(C_o - C_e)V}{m} \quad (2)$$

where V is the volume of dye solution (L) and m is the mass of the adsorbent (g).

3. Results and discussion

3.1. Characterisation of ZON

The XRD pattern of ZON synthesized by hydrothermal method was analysed by diffraction angle (2θ) and peaks intensity. The characteristic diffraction peaks at 2θ are 32.1°, 34.8°, 36.6°, 47.9°, 56.9°, 63.1°, 66.7°, 68.2°, 69.4° which resemble the diffraction plane (100), (002), (101), (102), (110), (103), (200), (112), (201) respectively as shown in Fig. 1. The observed diffraction

Table 1
Properties and structure of Victoria Blue B dye.

Dye	Victoria Blue B
Molecular formula and structure	$C_{33}H_{32}ClN_3$ 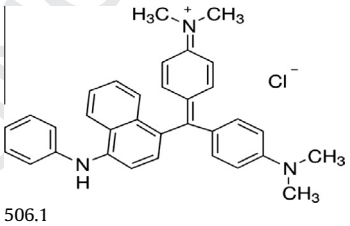
Molecular weight (g/mol)	506.1
Classification	Basic dye
C.I. no	44045
C.I. name	Basic blue 26
Melting point (°C)	206
Dye content (%)	85%
λ_{max} (nm)	599
Physical state	Dark blue to brown powder

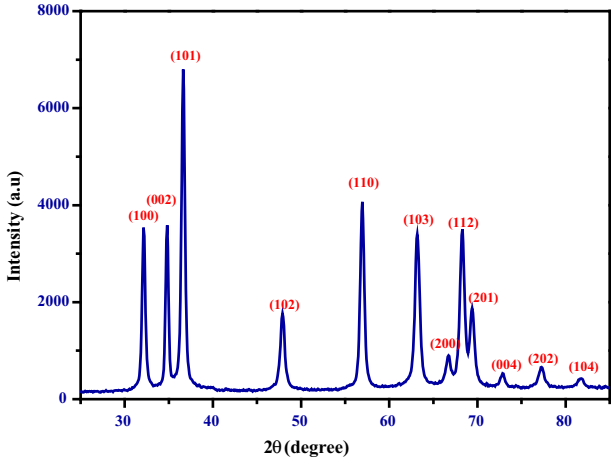

Fig. 1. X-ray diffraction patterns of synthesized ZON.

Please cite this article in press as: N. Kataria et al., Preparation, characterization and potential use of flower shaped Zinc oxide nanoparticles (ZON) for the adsorption of Victoria Blue B dye from aqueous solution, Advanced Powder Technology (2016), http://dx.doi.org/10.1016/j.apt.2016.04.001

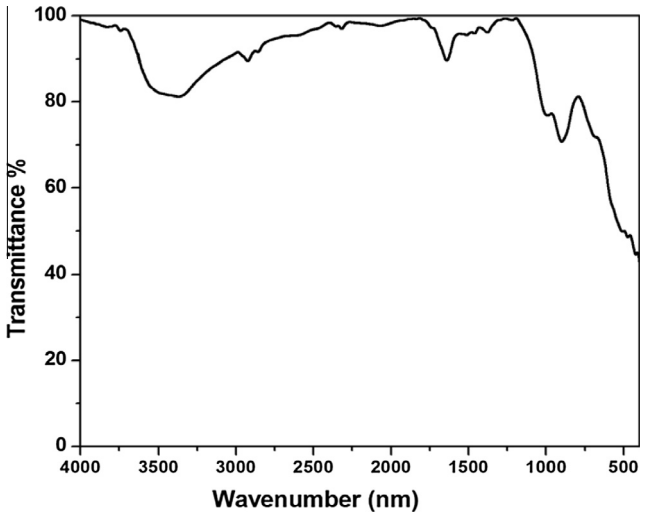

Fig. 2. FTIR spectra of synthesized ZON.

peaks of ZON in XRD pattern are in accordance with standard and reference XRD pattern of ZON revealed by the international centre for diffraction data [18]. Thus, the synthesized ZON represents hexagonal crystal structure. The lattice parameter was calculated from *d*-interplanar spacing of diffraction peak by following equation:

$$\frac{1}{d_{hkl}^2} = \frac{4}{3}\left(\frac{h^2 + hk + k^2}{a^2}\right) + \frac{l^2}{c^2} \quad (3)$$

The mean value of $a = 3.24$ and $c = 5.20$ Å calculated from the above equation also illustrated hexagonal structure of ZON [19].

FTIR (Fourier Transform Infrared) spectroscopy is an effective technique to observe the functional groups attached on the surface of synthesized ZON (Fig. 2). The strong and broad adsorption band at 3300–3450 cm^{-1} was assigned to O–H (hydroxyl group) stretching vibration due to presence of water. The symmetric and asymmetric stretching vibration peak of C–H bond was observed at ~2900 cm^{-1}. The weak peak at ~2200 cm^{-1} corresponded to C–N stretching vibration. Two bending vibration peaks around 1700 cm^{-1} and 900 cm^{-1} appeared due to O–H and C–H group respectively. The sharp absorption peak at 400–500 cm^{-1} revealed the presence of Zn–O stretching vibration thus confirming the synthesis of ZON [20].

The surface topography and morphology of ZON was studied by Scanning Electron Microscope (SEM) at 5000, 11,000, 20,000 and 40,000× magnification (Fig. 3a–d). The SEM results of the synthesized ZON clearly indicated the flower-shaped nanocrystals formed by agglomeration via hydrothermal route. The elemental composition of ZON was determined using Energy Dispersive X-Ray spectroscopy (Fig. 4) and it was found to be Zn and O element as 71.23% and 28.77% weight (%) and 37.74% and 62.26% respectively by atomic weight (%). No other element energy peak was detected in the EDX spectra.

DLS (Dynamic Light Scattering) is well established technique to measure the hydrodynamic diameter of synthesized ZON colloidal crystals. The average diameter of synthesised ZON ranges from 600 to 800 dnm as observed by the DLS data (Fig. 5).

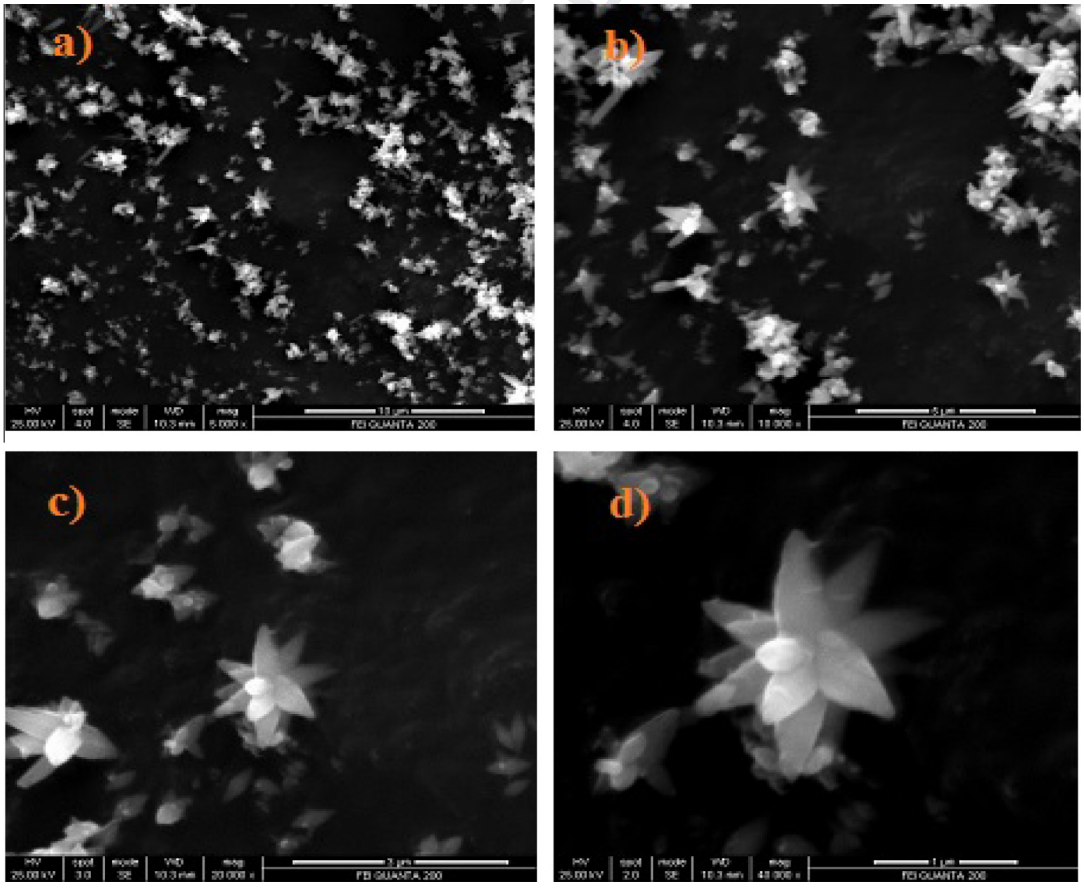

Fig. 3. (a–d) SEM image of synthesized ZON at different magnification.

Please cite this article in press as: N. Kataria et al., Preparation, characterization and potential use of flower shaped Zinc oxide nanoparticles (ZON) for the adsorption of Victoria Blue B dye from aqueous solution, Advanced Powder Technology (2016), http://dx.doi.org/10.1016/j.apt.2016.04.001

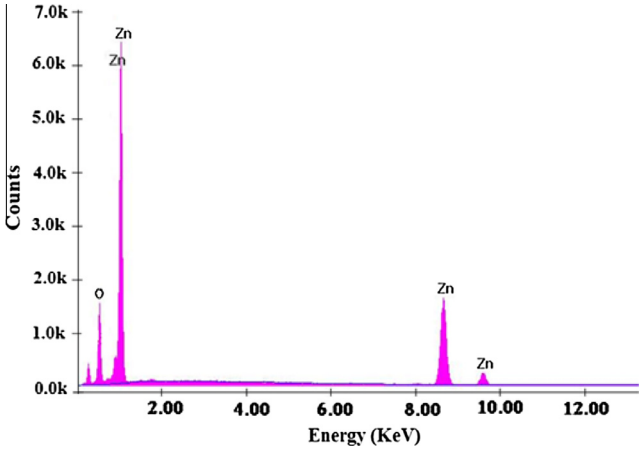

Fig. 4. EDX spectrum peaks of ZON.

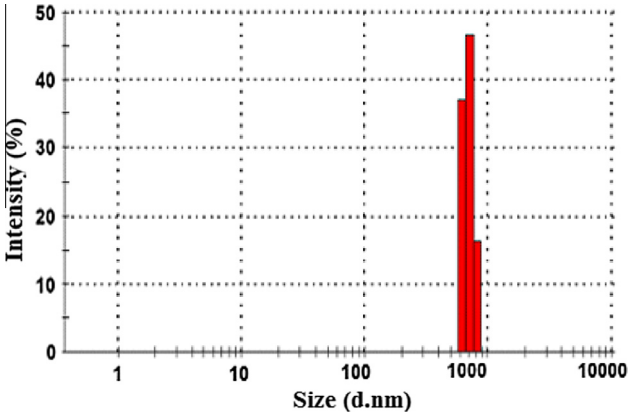

Fig. 5. DLS pattern of synthesized ZON.

3.2. Effect of pH

In adsorption experiments, pH is an important parameter to study the surface interaction between dye and adsorbent. The effect of pH (2–10) was studied using 0.04 g/100 mL of adsorbent dose at 50 mg/L dye concentration in 250 mL Erlenmeyer flasks at 27 ± 1 °C temperature for 90 min at a shaking speed of 180 rpm (Fig. 6). The results showed the dye removal increased up to 80% with increase in pH from 2 to 6. The maximum removal was achieved at pH 6, after that, it decreased with increase in pH from 6 to 10. At higher pH, change in colour of the dye has been observed. At lower pH, both cationic dye (VB B) and H^+ ions present in solution compete with each other for adsorption on the active sites of the nanoadsorbent thus, leading to less removal [21].

3.3. Effect of contact time on dye removal

The effect of contact time (15–120 min) on adsorption of VB B dye (10–100 mg/L) by ZON was studied by keeping all other process parameter as a constant. The adsorption of dye increased sharply up to 15 min of initiation of experiment (Fig. 7). After that, there was a slight increase in adsorption with increase in time and equilibrium was attained within 90 min. This may be reduction in surface area availability to VB B dye with time. Initially, rapid adsorption of dye molecule may be due to more free surface area availability are present, but after some time adsorption slows down as most of the surface area is covered by the dye molecules and no more sites are available for dye adsorption.

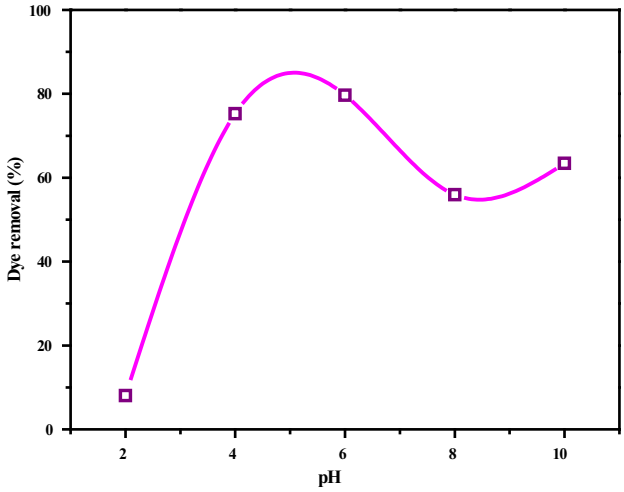

Fig. 6. Effect of pH on removal of 50 mg/L VB B dye by ZON.

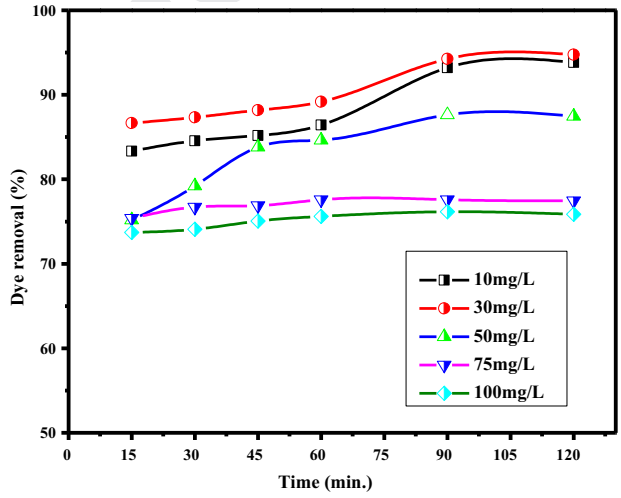

Fig. 7. Effect of contact time on adsorption of different VB B dye oncentration.

3.4. Effect of adsorbent dose on dye removal

The adsorbent dose and dye removal rate are economically very important parameter for industrial effluent treatment process. The effect of ZON dose on the removal of VB B dye was studied in the range of 0.02–0.10 g/100 mL) keeping all other variables constant. At low dye concentration (⩽30 mg/L) the dye removal increased from 80% to 96% with the increase in adsorbent dose from 0.02 to 0.10 g/100 mL and reached equilibrium at an adsorbent dose of 0.08 g/100 mL (Fig. 8). At higher concentration, the dye removal percentage was continuously increased with the increase in dose from 0.02 to 0.10 g/100 mL. Increase in dye removal with adsorbent dose may be attributed to increased surface area and availability of more adsorption sites.

3.5. Effect of temperature

The effect of temperature was studied for adsorption of VB B dye onto 0.04 g/100 mL adsorbent at pH 6.0 for 90 min. The adsorption experiments were performed in the temperature range of 10–70 °C. The dye removal increased from 68% to 97% with the increase in temperature and hence process was found to be endothermic in nature (Fig. 9). The dispersion and mobility of

Please cite this article in press as: N. Kataria et al., Preparation, characterization and potential use of flower shaped Zinc oxide nanoparticles (ZON) for the adsorption of Victoria Blue B dye from aqueous solution, Advanced Powder Technology (2016), http://dx.doi.org/10.1016/j.apt.2016.04.001

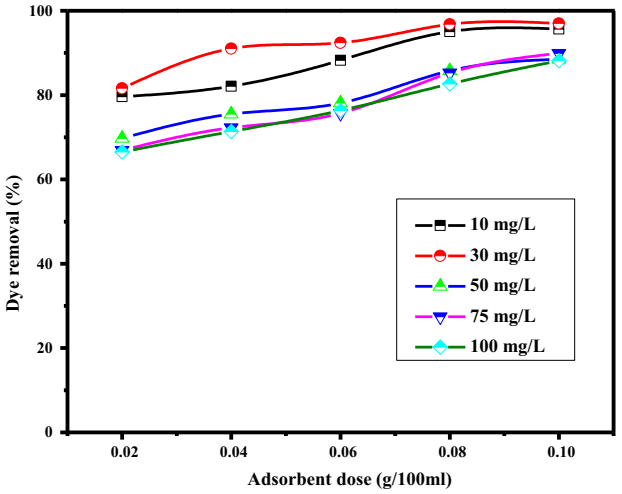

Fig. 8. Effect of adsorbent dose on removal of different VB B dye oncentration.

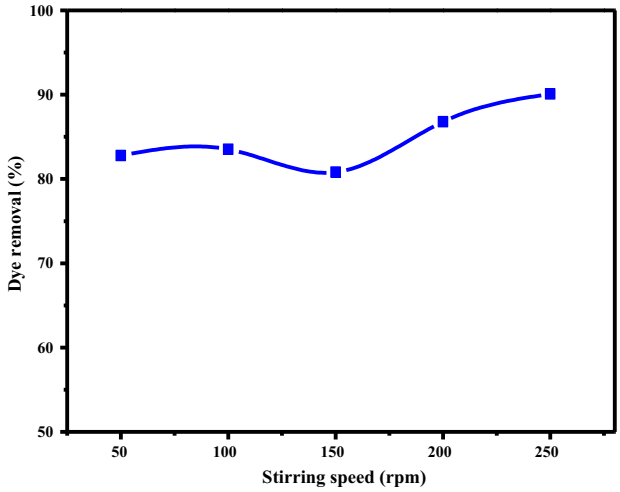

Fig. 10. Effect of stirring speed on removal of VB B dye.

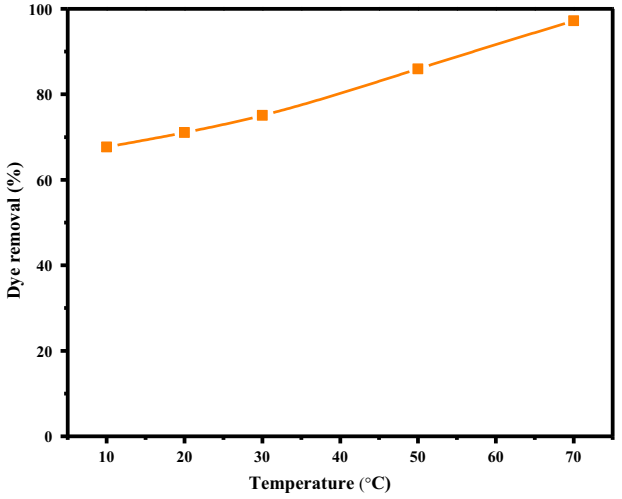

Fig. 9. Effect of temperature on adsorption of VB B dye.

dye molecules in solution increase with rise in temperature. Therefore, the rate of interaction between dye molecule and active site of adsorbent was increased which result into more adsorption at higher temperature [22]. Although, the rate of adsorption increased with increase in temperature, but all the adsorption experiments were carried out at room temperature.

3.6. Effect of stirring speed

The influence of stirring speed for adsorption of dye (50 mg/L) onto adsorbent dose (0.04 g/100 mL) was studied at 27 ± 1 °C for 90 min (Fig. 10). The dye removal was increased from 82% to 90% with increase in stirring speed form 50 rpm to 250 rpm beyond optimum stirring speed there was no effect on dye adsorption [23].

3.7. Thermodynamic study

The thermodynamic properties were investigated by experimental data obtained from adsorption experiments of VB B onto ZON at different temperature (10–70 °C) keeping all other variables constant. Thermodynamic parameters including change in Gibb's free energy (ΔG^0), enthalpy (ΔH^0), and entropy (ΔS^0) were determined by Vent Hoff Equation [24]

Table 2
Thermodynamic parameter for VB B dye adsorption over ZON.

T (K)	ΔG^0 (kJ mol^{-1})	ln(K_d)	ΔS^0 (J mol^{-1} K^{-1})	ΔH^0 (kJ mol^{-1})
283	−1.741	0.7399	29.743	1.673
293	−2.189	0.8987		
303	−2.780	1.1036		
323	−4.865	1.8116		
343	−10.106	3.5439		

$$\Delta G^0 = -RT \ln K_d \quad (4)$$

where ΔG^0 (kJ mol^{-1}) is the change in free energy, R is gas constant (8.314 J mol^{-1} K^{-1}), T is the temperature (K) and K_d is the equilibrium constant expressed by following equation

$$K_d = \frac{C_a}{C_e} \quad (5)$$

where C_a is the amount of dye concentration on adsorbent at equilibrium. The standard Gibb's free energy changes are also represented by following equations:

$$\Delta G^0 = \Delta H^0 - T\Delta S^0 \quad (6)$$

$$\ln K_d = \frac{\Delta H^0}{RT} - \frac{\Delta S^0}{R} \quad (7)$$

where ΔH^0 (kJ mol^{-1}) and ΔS^0 (J mol^{-1} K^{-1}) are enthalpy and entropy respectively. The value of ΔS^0 and ΔS^0 were calculated from the slope and intercept respectively obtained from plot between ln K_d versus $1/T$. The negative values of ΔG^0 determined from the adsorption experiments revealed the feasibility and spontaneity of VB B dye adsorption onto ZON with increase in temperature from 10 °C to 70 °C and the positive value of ΔH^0 indicate the adsorption process was endothermic in nature (Table 2). The positive value of ΔS^0 explained the affinity of adsorbent for VB B and increase randomness during adsorption experiment [25].

3.8. Adsorption isotherm models

The adsorption isotherms justify the adsorption behaviour or interaction between the soluble phase (liquid) and insoluble phase (solid) in the system. The adsorption equilibrium of VB B dye onto ZON was studied under various adsorption experiments and adsorption data was explained by mainly three adsorption

Please cite this article in press as: N. Kataria et al., Preparation, characterization and potential use of flower shaped Zinc oxide nanoparticles (ZON) for the adsorption of Victoria Blue B dye from aqueous solution, Advanced Powder Technology (2016), http://dx.doi.org/10.1016/j.apt.2016.04.001

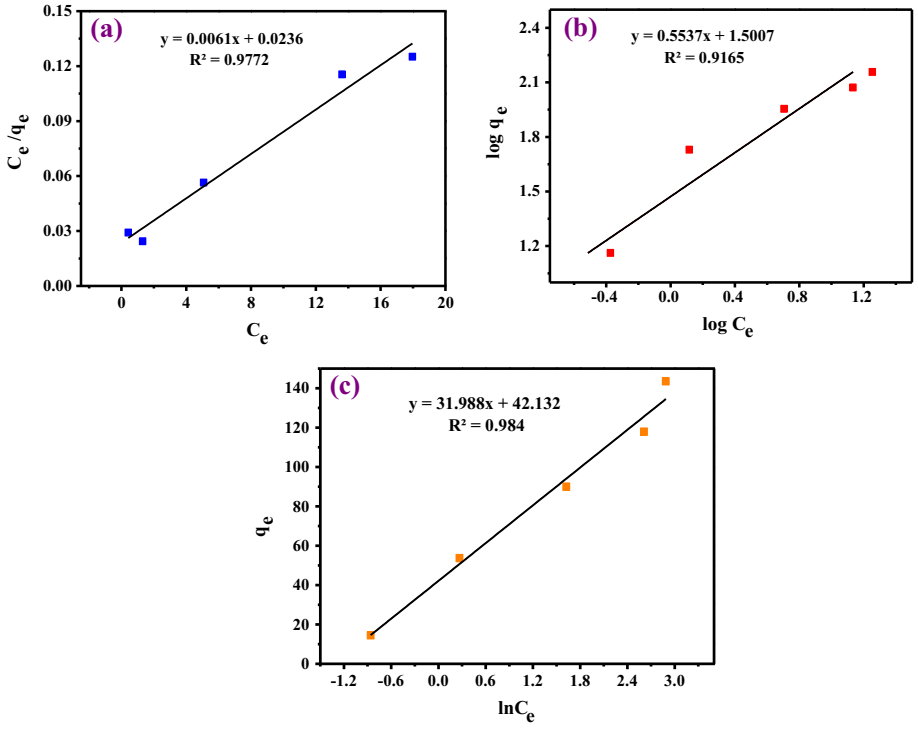

Fig. 11. Adsorption isothermal models plots for VB B dye adsorption on ZON (a) Langmuir isotherm plot, (b) Freundlich isotherm plot and (c) Temkin isotherm plot.

Table 3
Various adsorptions isothermal model for VB B dye adsorption interpreted by correlation coefficients and adsorption parameters.

Isotherms model	Linear equation	Parameters	Values
Langmuir	$C_e/q_e = 1/q_{max}b + C_e/q_{max}$	q_{max} (mg/g)	163.93
		b (L/mg)	0.258
		R^2	0.977
		R_L	0.072
		C_o (mg/L)	50
Freundlich	$\log q_e = \log K_f + 1/n \log C_e$	$1/n$	0.554
		K_f (mg/g)	31.67
		R^2	0.916
Temkin	$q_e = B \ln K_T + B \ln C_e$	B	31.988
		K_T (L/g)	3.732
		R^2	0.982

isotherm models i.e. Langmuir, Freundlich and Temkin. Langmuir adsorption model assumes monolayer distribution of dye at a specific homogeneous site within the adsorbent surface [26].

Langmuir model can be written in a linear form as represented in Eq. (8)

$$\frac{C_e}{q_e} = \frac{1}{q_{max}b} + \frac{C_e}{q_{max}} \quad (8)$$

where q_{max} (mg/g) is the maximum monolayer adsorption capacity, b (L/mg) is the Langmuir constant related to the affinity of binding sites. The linear plot was obtained between C_e/q_e vs C_e (Fig. 11a). Adsorption model parameters and correlation coefficient (R^2) were calculated and are given Table 3. The essential characteristics of the Langmuir isotherm can be explained by the dimensionless constant [27] which is called equilibrium parameter R_L expressed as Eq. (9)

$$R_L = \frac{1}{1 + bC_O} \quad (9)$$

where R_L value indicates the isotherm to be either favourable ($0 < R_L < 1$) or unfavourable ($R_L > 1$).

Freundlich isotherm model is based on the assumption that adsorption of adsorbate molecules occurs in multilayer. The distribution of active site on the adsorbent surface is energetically heterogeneous in nature.

A linear form of model is represented in Eq. (10)

$$\log q_e = \log K_f + \frac{1}{n} \log C_e \quad (10)$$

where K_f (mg/g(L/mg)$^{1/n}$) is Freundlich constant related to adsorption capacity and n is the heterogeneity factor related to intensity of adsorption. The value of K_f and n were calculated from the linear plot between $\log q_e$ versus $\log C_e$ as shown in Fig. 11(b). The value of n should lie in between 1 and 10 for favourable adsorption [28,29].

Temkin & Pyzhev isotherm model [30] is mainly based on the assumption that (i) there is monolayer distribution of adsorbate on heterogeneous active sites on the adsorbent surface or (ii) there is uniform distribution of binding energy and due to interaction between adsorbate and adsorbent, the heat of adsorption of adsorbed dye molecule decreases linearly with coverage. A linear form of model is expressed by Eq. (11).

$$q_e = B \ln K_T + B \ln C_e \quad (11)$$

where $B = RT/b$, b is the Temkin constant related to heat of adsorption (J mol^{-1}) and K_T is equilibrium binding constant (L/g). The value of K_T and B was calculated by plotting the graph between q_e vs $\ln C_e$ (Fig. 11c).

By comparing the isotherm models, it was found that the data fitted well to Langmuir and Temkin models, with a high correlation coefficient (R^2) value of 0.977 and 0.984 respectively while Freundlich isotherm model ($R^2 < 0.95$) did not fit the experimental data (Table 3). This may be due to the monolayer distribution of basic dye on the homogeneous as well as heterogeneous active sites present on the ZON crystals surface. The adsorption capacity of various types of Zinc oxide particles has been encapsulated in

Please cite this article in press as: N. Kataria et al., Preparation, characterization and potential use of flower shaped Zinc oxide nanoparticles (ZON) for the adsorption of Victoria Blue B dye from aqueous solution, Advanced Powder Technology (2016), http://dx.doi.org/10.1016/j.apt.2016.04.001

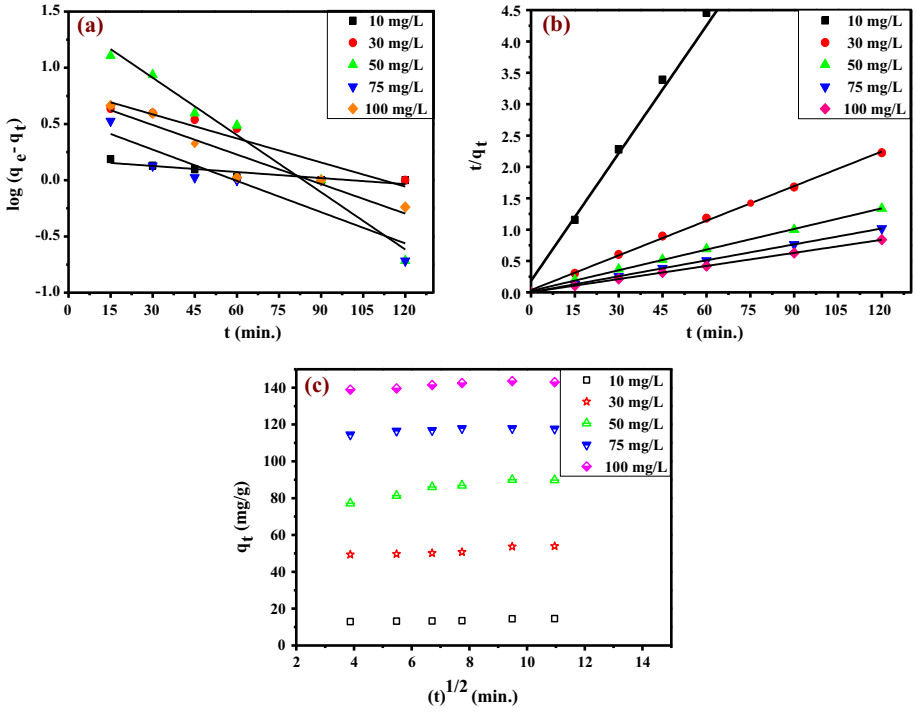

Fig. 12. Kinetic models plots for VB B dye adsorption by ZON. (a) Pseudo-first order plot, (b) pseudo-second order plot and (c) intraparticle diffusion plot.

Table 4
Comparative adsorption capacity of various ZnO particles for dyes removal from aqueous solution.

Adsorbent	Dyes removed	q_e (mg/g)	Reference
Zinc oxide nanoparticle (ZON)	Acid Blue 25	20	[34]
	Direct Red 23	12	
	Direct Red 31	15	
Amine-functionalised zinc oxide nanoparticles (AFZON)	Acid Blue 25	1250	[34]
	Direct Red 23	1000	
	Direct Red 31	1429	
Zinc oxide nanoparticles loaded on activated carbon (ZNO-NP-AC)	Brilliant green	142.9	[35]
ZnO nanoparticles	Malachite green oxalate	310.5	[36]
Zinc oxide nanoparticles loaded on activated carbon (ZnO-NP-AC)	Malachite green	76.92–322.58	[37]
Zinc oxide nanoparticles loaded on activated carbon (ZnO-NP-AC)	Bromophenol red	200	[38]
ZnS:Mn nanoparticles loaded on activated carbon	Direct Yellow 12	90.05	[39]
	Reactive Orange 12	94.52	
$Zn(OH)_2$ nanoparticles-activated carbon	Sunset yellow	84.74–158.7	[40]
ZnS:Cu nanoparticles loaded on activated carbon	Reactive Orange 12	193.5–382.8	[41]
	Direct yellow 12	153.9–325.3	
Flower-shaped Zinc oxide nanoparticles (ZON)	Victoria Blue B	163.93	This study

Table 4. The data shows that adsorption capacity of ZON is comparable with other material.

3.9. Kinetic study

The rate controlling step or mechanism of adsorption of VB B dye onto the flower shaped ZON was explained by adsorption kinetic models such as pseudo-first order, pseudo-second order and intraparticle diffusion. Lagergren pseudo-first order model is represented in the linear form given in Eq. (12).

$$\log(q_e - q_t) = \log q_e - \left(\frac{k_1}{2.303}\right)t \tag{12}$$

where q_t (mg/g) are the adsorption capacity at time t and k_1 (min^{-1}) is the kinetic rate constant. The value of pseudo-first order kinetic constant, k_1 and q_e was calculated from linear plot between $\log(q_e - q_t)$ versus t (Fig. 12a). The dye adsorption did not follow the pseudo-first order model as the R^2 value was smaller than pseudo second order model (0.984) and q_e (cal) values did not match q_e (exp) values (Table 4).

A linear form of pseudo-second order model is given in Eq. (13) [32].

$$\frac{t}{q_t} = \frac{1}{k_2 q_e^2} + \frac{t}{q_e} \tag{13}$$

where k_2 (g/mg min) is the rate constant of the pseudo-second order. The value of k_2 and q_e was determined by plotting the graph between t/q_t versus t (Fig. 12b). The pseudo-second order model is in good agreement with adsorption process with a very high correlation coefficient $R^2 \geqslant 0.997$ and q_e (cal) values are almost equivalent to q_e (exp) values obtained from adsorption experiment.

The possibility of intraparticle diffusion is explained by intraparticle diffusion model [32]. The intraparticle diffusion model is expressed by Eq. (14).

Please cite this article in press as: N. Kataria et al., Preparation, characterization and potential use of flower shaped Zinc oxide nanoparticles (ZON) for the adsorption of Victoria Blue B dye from aqueous solution, Advanced Powder Technology (2016), http://dx.doi.org/10.1016/j.apt.2016.04.001

Table 5
Kinetic models parameter study at various concentration of VB B dye adsorption on ZON.

Kinetic models	Parameters	Values of parameters				
		10 mg/L	30 mg/L	50 mg/L	75 mg/L	100 mg/L
Pseudo-first order	k_1 (min^{-1})	0.0041	0.0164	0.0389	0.0212	0.0200
	q_e (cal)	1.516	6.310	26.31	3.55	5.677
	R^2	0.8299	0.9010	0.9836	0.8141	0.9071
Pseudo-second order	k_2 (g/mg min)	0.02492	0.00905	0.00516	0.03261	0.01597
	q_e (cal)	14.749	54.348	91.158	118.064	143.266
	R^2	0.9975	0.9986	0.9992	0.9999	0.9999
Intraparticle diffusion	k_{id} (mg g^{-1} $min^{-1/2}$)	0.2587	0.7383	1.8383	0.4256	0.6699
	C	11.7620	45.8218	71.6685	113.7522	136.5664
	R^2	0.8883	0.8992	0.8998	0.7299	0.8635
Experimental data	q_e (exp)	14.62	53.94	90.00	117.88	143.56

$$q_t = k_{id}t^{1/2} + C \quad (14)$$

where q_t (mg/g) is the equilibrium dye uptake at time t, k_{id} (mg g^{-1} $min^{-1/2}$) is the intra-particle diffusion rate constant and C (mg/g) is the intercept showing the thickness of boundary layer effect. The value of k_{id} and C were calculated from the plot between q_t versus k_{id} (Fig. 12c). If the plot doesn't pass through the origin ($C \neq 0$), then intraparticle diffusion is the only rate controlling step. In the present kinetic study, the correlation coefficient (R^2) value is comparatively low (<0.899) as indicated by Table 5 thus, showing that the intraparticle diffusion model is insignificant for adsorption experiments [33]. In the adsorption process, pseudo-second order model was well suited as compared to pseudo-first order and intra-particle diffusion models due to their high correlation coefficient.

4. Conclusion

Flower shaped ZON synthesized by hydrothermal method at 80–90 °C during chemical process has good adsorption efficiency for VB B adsorption. The properties of ZON like crystal structure, morphology, elemental composition and particle size were illustrated by XRD, SEM, EDX and DLS respectively. The maximum adsorption capacity of VB B dye 163.93 mg/g was calculated by Langmuir model. The monolayer adsorption and homogenous active sites were explained by the Langmuir and Temkin isotherm models. The rate of adsorption of VB B dye is in good agreement with pseudo-second order model. The adsorption process is spontaneous, favourable and endothermic in nature verified by thermodynamic study. Hence, it can be concluded that flower shape ZON can be good adsorbent for some other basic dyes as well.

5. Uncited reference

[31].

Acknowledgement

One of the authors' N. Kataria is thankful to UGC, New Delhi, India for providing financial assistance as Junior Research Fellowship.

References

[1] G. McKay, M.S. Otterburn, A.G. Sweeney, The removal of colour from effluent using various adsorbents. III. Silica: rate process, Water Res. 14 (1980) 15–20.
[2] G. Moussavi, M. Mahmoudi, Removal of azo and anthraquinone reactive dyes from industrial wastewaters using MgO nanoparticles, J. Hazard. Mater. 168 (2009) 806–812.
[3] Reife, H.S. Fremann, Environmental Chemistry of Dyes and Pigments, Wiley, New York, 1996.
[4] Z.Q. Zhang, X.Q. Xu, Flow-injection catalytic spectrophotometric determination of oxalic acid using the redox reaction between Victoria blue B and dichromate, Anal. Chim. Acta 406 (2000) 303–308.
[5] J.F. Riley, Retardation of growth of a transplantable carcinoma in mice fed basic metachromatic dyes, Cancer Res. 8 (1948) 183–188.
[6] E. Schulte, D. Wittekind, V. Kretschmer, Victoria blue B—a nuclear stain for cytology. A cytophotometric study, Histochemistry 88 (1988) 427–433.
[7] V.K. Garg, M. Amita, R. Kumar, R. Gupta, Basic dye (methylene blue) removal from simulated wastewater by adsorption using Indian Rosewood sawdust: a timber industry waste, Dyes Pigm. 63 (2004) 243–250.
[8] S.A. Avlonitis, I. Poulios, D. Sotiriou, M. Pappas, K. Moutesidis, Simulated cotton dye effluents treatment and reuse by nano filtration, Desalination 221 (2008) 259–267.
[9] W.J. Lau, A.F. Ismail, Polymeric nanofiltration membranes for textile dye wastewater treatment: preparation, performance evaluation, transport modelling, and fouling control—a review, Desalination 245 (2009) 321–348.
[10] X. Di, S.K. Kansal, W. Deng, Preparation, characterization and photocatalytic activity of flowerlike cadmium sulfide nanostructure, Sep. Purif. Technol. 68 (2009) 61–64.
[11] S.A. Wang, Comparative study of Fenton and Fenton-like reaction kinetics in decolourisation of wastewater, Dyes Pigm. 76 (2008) 714–720.
[12] R.Y.L. Yeh, A. Thomas, Color removal from dye wastewaters by adsorption using powdered activated carbon: mass transfer studies, J. Chem. Technol. Biotechnol. 63 (1995) 48–54.
[13] T.V. Rêgo, T.R.S. Cadaval Jr., G.L. Dotto, L.A.A. Pinto, Statistical optimization, interaction analysis and desorption studies for the azo dyes adsorption onto chitosan films, J. Colloid Interface Sci. 411 (2013) 27–33.
[14] V.K. Garg, R. Kumar, R. Gupta, Removal of malachite green dye from aqueous solution by adsorption using agro-industry waste: a case study of *Prosopis cineraria*, Dyes Pigm. 62 (2004) 1–10.
[15] Y.J. Wu, L.J. Zhang, C.L. Gao, J.Y. Ma, X.H. Ma, R.P. Han, Adsorption of copper ions and methylene blue in a single and binary system on wheat straw, J. Chem. Eng. Data 54 (2009) 3229–3234.
[16] S.K. Kansal, M. Singh, D. Sud, Studies on photodegradation of two commercial dyes in aqueous phase using different photocatalysts, J. Hazard. Mater. 141 (2007) 581–590.
[17] N. Modirshahla, A. Hassani, M.A. Behnajady, R. Rahbarfam, Effect of operational parameters on decolorization of Acid Yellow 23 from wastewater by UV irradiation using ZnO and ZnO/SnO_2 photocatalysts, Desalination 271 (2011) 187–192.
[18] M.F. Khan, M. Hameedullah, A.H. Ansari, E. Ahmad, M.B. Lohani, R.H. Khan, M. M. Alam, W. Khan, F.M. Husain, I. Ahmad, Flower shaped ZnO nanoparticle from synthesized by a novel approach at near-room temperatures with antibacterial and antifungal properties, Int. J. Nanomed. 9 (2014) 853–864.
[19] U.K. Gautam, L.S. Panchakarla, B. Dierre, X. Fang, Y. Bando, T. Sekiguchi, A. Govindaraj, D. Golberg, C.N.R. Rao, Solvothermal synthesis, cathodoluminescence, and field-emission properties of pure and n-doped ZnO nanobullets, Adv. Funct. Mater. 19 (2009) 131–140.
[20] S.K. Kansal, R. Lamba, S.K. Mehta, A. Umar, Photocatalytic degradation of Alizarin Red S using simply synthesized ZnO nanoparticles, Mater. Lett. 106 (2013) 385–389.
[21] B.H. Hameed, D.K. Mahmoud, A.L. Ahmad, Equilibrium modelling and kinetic studies on the adsorption of basic dye by a low cost adsorbent: coconut (*Cocos nucifera*) bunch waste, J. Hazard. Mater. 158 (2008) 65–72.
[22] M. Ghosh, C.N.R. Rao, Solvothermal synthesis of CdO and CuO nanocrystals, Chem. Phys. Lett. 393 (2004) 493–497.
[23] M. Alkan, M. Dogan, Y. Turhan, O. Demirbas, P. Turan, Adsorption kinetics and mechanism of maxilon blue 5G dye on sepiolite from aqueous solutions, Chem. Eng. J. 139 (2008) 213–223.
[24] J.M. Smith, H.C.V. Ness, Introduction to Chemical Engineering Thermodynamics, McGraw-Hill New York, USA, 1987.
[25] M.H. Do, N.H. Phan, T.D. Nguyen, T.T.S. Pham, V.K. Nguyen, T.T.T. Vu, T.K.P. Nguyen, Activated carbon/Fe_3O_4 nanoparticle composite: fabrication, methyl orange removal and regeneration by hydrogen peroxide, Chemosphere 85 (2011) 1269–1276.

[26] I. Langmuir, The constitution and fundamental properties of solids and liquid, J. Am. Chem. Soc. 38 (1916) 2221–2295.
[27] R. Sivaraj, C. Namasivayam, K. Kadirvelu, Orange peel as an adsorbent in the removal of Acid Violet 17 (acid dye) from aqueous solutions, Waste Manage. 21 (2001) 105–110.
[28] H.M.F. Freundlich, Over the adsorption in solution, J. Phys. Chem. 57 (1906) 385–471.
[29] C. Namasivayam, K. Kadirvelu, Agricultural solid wastes for the removal of heavy metals: adsorption of Cu (II) by coir pith carbon, Chemosphere 34 (1997) 377–399.
[30] M.J. Temkin, V. Pyzhev, Recent modification to Langmuir isotherms, Acta Physiochim. USSR 12 (1940) 217–222.
[31] Y.S. Ho, G. McKay, Pseudo-second order model for sorption processes, Process Biochem. 34 (1999) 451–465.
[32] W.J. Weber, J.C. Morris, Kinetics of adsorption on carbon from solution, J. Sanitary Eng. Div. Am. Soc. Civ. Eng. 89 (1963) 31–60.
[33] L. Fan, C. Luo, X. Li, F. Lu, H. Qiu, M. Sun, Fabrication of novel magnetic chitosan grafted with graphene oxide to enhance adsorption properties for methyl blue, J. Hazard. Mater. 215–216 (2012) 272–279.
[34] N.M. Mahmoodia, F. Najafib, Preparation of surface modified zinc oxide nanoparticle with high capacity dye removal ability, Mater. Res. Bull. 47 (2012) 1800–1809.
[35] M. Ghaedi, G. Negintaji, H. Karimi, F. Marahe, Solid phase extraction and removal of brilliant green dye on zinc oxide nanoparticles loaded on activated carbon: new kinetic model and thermodynamic evaluation, J. Ind. Eng. Chem. 20 (2013) 1444–1452.
[36] K.Y. Kumar, H.B. Muralidhara, Y.A. Nayaka, J. Balasubramanyam, H. Hanumanthappa, Low-cost synthesis of metal oxide nanoparticles and their application in adsorption of commercial dye and heavy metal ion in aqueous solution, Powder Technol. 246 (2013) 125–136.
[37] M. Ghaedi, A. Ansari, M.H. Habibi, A.R. Asghari, Removal of malachite green from aqueous solution by zinc oxide nanoparticle loaded on activated carbon: kinetics and isotherm study, J. Ind. Eng. Chem. 20 (2014) 17–28.
[38] M. Ghaedi, M. Ghayedi, S.N. Kokhdan, R. Sahraei, A. Daneshfar, Palladium, silver, and zinc oxide nanoparticles loaded on activated carbon as adsorbent for removal of bromophenol red from aqueous solution, J. Ind. Eng. Chem. 19 (2013) 1209–1217.
[39] S. Hajati, M. Ghaedi, F. Karimi, B. Barazesh, R. Sahraei, A. Daneshfar, Competitive adsorption of Direct Yellow 12 and Reactive Orange 12 on ZnS: Mn nanoparticles loaded on activated carbon as novel adsorbent, J. Ind. Eng. Chem. 20 (2014) 564–571.
[40] M. Ghaedi, A.M. Ghaedi, E. Negintaji, A. Ansari, F. Mohammadi, Artificial neural network – imperialist competitive algorithm based optimization for removal of sunset yellow using $Zn(OH)_2$ nanoparticles-activated carbon, J. Ind. Eng. Chem. 20 (2014) 4332–4343.
[41] M. Ghaedi, A. Ansari, R. Sahraei, ZnS:Cu nanoparticles loaded on activated carbon as novel adsorbent for kinetic, thermodynamic and isotherm studies of Reactive Orange 12 and Direct yellow 12 adsorption, Spectrochim. Acta Part A: Mol. Biomol. Spectrosc. 114 (2013) 687–694.

Please cite this article in press as: N. Kataria et al., Preparation, characterization and potential use of flower shaped Zinc oxide nanoparticles (ZON) for the adsorption of Victoria Blue B dye from aqueous solution, Advanced Powder Technology (2016), http://dx.doi.org/10.1016/j.apt.2016.04.001